

This copy is for your personal, non-commercial use only.

If you wish to distribute this article to others, you can order high-quality copies for your colleagues, clients, or customers by [clicking here](#).

Permission to republish or repurpose articles or portions of articles can be obtained by following the guidelines [here](#).

The following resources related to this article are available online at www.sciencemag.org (this information is current as of November 3, 2010):

Updated information and services, including high-resolution figures, can be found in the online version of this article at:

<http://www.sciencemag.org/cgi/content/full/314/5796/136>

Supporting Online Material can be found at:

<http://www.sciencemag.org/cgi/content/full/314/5796/136/DC1>

A list of selected additional articles on the Science Web sites **related to this article** can be found at:

<http://www.sciencemag.org/cgi/content/full/314/5796/136#related-content>

This article **cites 26 articles**, 14 of which can be accessed for free:

<http://www.sciencemag.org/cgi/content/full/314/5796/136#otherarticles>

This article has been **cited by** 13 article(s) on the ISI Web of Science.

This article has been **cited by** 3 articles hosted by HighWire Press; see:

<http://www.sciencemag.org/cgi/content/full/314/5796/136#otherarticles>

This article appears in the following **subject collections**:

Immunology

<http://www.sciencemag.org/cgi/collection/immunology>

16. A. H. Peden, M. W. Head, D. L. Ritchie, J. E. Bell, J. W. Ironside, *Lancet* **364**, 527 (2004).
17. M. Glatzel, E. Abela, M. Maissen, A. Aguzzi, *N. Engl. J. Med.* **349**, 1812 (2003).
18. M. W. Miller, E. S. Williams, *Curr. Top. Microbiol. Immunol.* **284**, 193 (2004).
19. C. DeJoia, B. Moreaux, K. O'Connell, R. A. Bessen, *J. Virol.* **80**, 4546 (2006).
20. M. P. Perrott, paper presented at the Molecular Mechanisms of Transmissible Spongiform Encephalopathies (Prion Diseases) Keystone Meeting, Snowbird, UT, 11 to 15 January 2005.
21. M. W. Miller, E. S. Williams, N. T. Hobbs, L. L. Wolfe, *Emerg. Infect. Dis.* **10**, 1003 (2004).
22. S. Supattapone *et al.*, *J. Virol.* **75**, 1408 (2001).
23. M. Jeffrey *et al.*, *J. Pathol.* **209**, 4 (2006).
24. C. Scherbel *et al.*, *Vet. Res.* **37**, 695 (2006).
25. S. R. Browning *et al.*, *J. Virol.* **78**, 13345 (2004).
26. E. S. Williams, M. W. Miller, *Rev. Sci. Tech.* **21**, 305 (2002).
27. We thank J. Grassi for his gift of PrP monoclonal antibody; M. Perrott for his technical expertise with the NaPTA methodology; K. O'Rourke and L. Hamburg for performing the PRNP genotype analysis; and C. Tedford for his expertise in deer behavior, facility design, and transport. We thank the office of the CSU Vice President for Research (A. Frank and K. Delehoj) for their support in establishing the CWD deer isolation facility. Animals

were housed and cared for in accordance to CSU Animal Care and Use Committee regulations. This work was supported by the NIH, National Institute of Allergy and Infectious Diseases, contract N01-AI-25491.

Supporting Online Material

www.sciencemag.org/cgi/content/full/314/5796/133/DC1
Material and Methods
SOM Text
Tables S1 and S2
References

18 July 2006; accepted 29 August 2006
10.1126/science.1132661

Modulation of Cell Adhesion and Motility in the Immune System by Myo1f

Sangwon V. Kim,^{1*} Wajahat Z. Mehal,^{1,3} Xuemei Dong,⁶ Volkmar Heinrich,^{7†} Marc Pypaert,^{4,5} Ira Mellman,^{4,5} Micah Dembo,⁷ Mark S. Mooseker,^{4,8} Dianqing Wu,^{6‡} Richard A. Flavell^{1,2§}

Although class I myosins are known to play a wide range of roles, the physiological function of long-tailed class I myosins in vertebrates remains elusive. We demonstrated that one of these proteins, Myo1f, is expressed predominantly in the mammalian immune system. Cells from Myo1f-deficient mice exhibited abnormally increased adhesion and reduced motility, resulting from augmented exocytosis of $\beta 2$ integrin-containing granules. Also, the cortical actin that co-localizes with Myo1f was reduced in Myo1f-deficient cells. In vivo, Myo1f-deficient mice showed increased susceptibility to infection by *Listeria monocytogenes* and an impaired neutrophil response. Thus, Myo1f directs immune cell motility and innate host defense against infection.

In both mouse and human genomes, 16 genes encode conventional class II muscle and non-muscle myosins, with 25 “unconventional” myosin genes encoding 11 other classes (1). Natural mutations of various myosin genes result in an array of genetic disorders, including cardiomyopathies, deafness, blindness, glomerular nephritis, and neuropathies (2, 3). The class I myosins are the largest group of unconventional myosins and are evolutionarily ancient, existing in a wide range of species from yeast to vertebrates (1, 4). Mice and humans have a total of eight class I myosin heavy-chain

genes, six of which encode short-tailed forms (Myo1a, b, c, d, g, and h) and two of which encode long-tailed (amoeboid) forms (Myo1e and f) (1). All class I myosins consist of an N-terminal motor domain, light-chain-binding IQ motifs, and a basic tail homology 1 (TH1) domain thought to affect interactions with membranes (2). The long-tailed class I myosins have an additional proline-rich TH2 domain and a TH3 domain containing a single Src homology 3 (SH3) domain (2).

The class I myosins in *Dictyostelium* and yeast are involved in migration, phagocytosis, endocytosis, and actin remodeling (5, 6). Short-tailed class I myosins in vertebrates are involved in more specialized functions, such as the adaptation of hair cells in the ear (7) and the transport of vesicles and organelles (8, 9), as well as the structural maintenance of the enterocyte microvilli (10). However, the function of long-tailed class I myosins in vertebrates is poorly characterized (11–14).

Myo1f was first identified in our screen for differentially expressed genes in subsets of murine lymphocytes. In contrast to previous data suggesting the widespread expression of Myo1f in tissues (15), our results, which we obtained using specific probes, showed that Myo1f is selectively expressed in the spleen, mesenteric lymph nodes, thymus, and lung (Fig. 1A). By comparison, specific detection of Myo1e showed

a predominant expression pattern in the spleen and mesenteric lymph nodes and moderate expression in the lung, small intestine, and large intestine (Fig. 1B). Within the lymphoid tissues, natural killer (NK) cells, macrophages, and dendritic cells were found to express considerable levels of both Myo1f and Myo1e; neutrophils and B cells showed selective expression of Myo1f and Myo1e, respectively (Fig. 1, C and D).

To determine the function of Myo1f in the vertebrate immune system, we generated Myo1f gene-deficient mice. We focused on neutrophils because Myo1f was detected exclusively in neutrophils (Fig. 1, C and D). Immunoglobulin G (IgG)-mediated phagocytosis was similar between wild-type and knockout (KO) neutrophils (Fig. 1E). To evaluate the degree of pathogen killing that follows phagocytosis, we measured the production of reactive oxygen species. Again, no considerable difference was detected between wild-type and KO neutrophils (Fig. 1F). Thus, Myo1f is dispensable for both the phagocytosis of bacteria and their destruction.

Integrin-mediated adhesion to the vascular endothelium is crucial in the process of neutrophil migration to infected tissue, and the dominant integrins involved in this process belong to the $\beta 2$ integrin (CD18) family (16). Myo1f-deficient neutrophils exhibited stronger adhesion to integrin ligands, including the intercellular adhesion molecule-1 (ICAM-1) (CD54) and fibronectin (Fig. 2, A and B). Activation of neutrophils by the proinflammatory cytokine tumor necrosis factor- α did not compensate for this difference, suggesting that increased adhesion did not result from changes in the activation status of Myo1f-deficient cells. Experiments with a blocking antibody showed that most of the adhesion was mediated by $\beta 2$ integrin (Fig. 2, A and B). In addition, Myo1f affected only integrin-mediated adhesion, not integrin-independent adhesion to polylysine-coated substrate (Fig. 2C) (17). Spreading of Myo1f-deficient neutrophils on ICAM-1 was also increased as compared to that of wild-type neutrophils (Fig. 2D). Increased spreading was not due to a loss of cortical tension (fig. S2), which acts to maintain the round shape of the cells (Fig. 2E). In contrast, myosin I double mutants in *Dictyostelium* exhibit abnormalities

¹Section of Immunobiology, ²Howard Hughes Medical Institute, ³Section of Digestive Diseases, ⁴Department of Cell Biology, ⁵Ludwig Institute for Cancer Research, Yale University School of Medicine, New Haven, CT 06520, USA. ⁶Department of Genetics and Developmental Biology, University of Connecticut Health Center, Farmington, CT 06030, USA. ⁷Department of Biomedical Engineering, Boston University, Boston, MA 02215, USA. ⁸Departments of Molecular, Cellular and Developmental Biology, and Department of Pathology, Yale University, New Haven, CT 06511, USA.

*Present address: Immunology Program, Memorial Sloan-Kettering Cancer Center, New York, NY 10021, USA.

†Present address: Department of Biomedical Engineering, University of California Davis, Davis, CA 95616, USA.

‡Present address: Vascular Biology and Transplantation Program and Department of Pharmacology, Yale University School of Medicine, New Haven, CT 06520, USA.

§To whom correspondence should be addressed. E-mail: richard.flavell@yale.edu

in surface morphology resulting from an inability to maintain a sufficient level of resting cortical tension (5, 18). Together, these results suggest that, in the absence of Myo1f, neutrophils are more adherent to $\beta 2$ integrin ligand.

Under resting conditions, no considerable difference was seen in the level of $\beta 2$ integrin on the surface of Myo1f-deficient cells (Fig. 3A). In neutrophils, a large pool of integrin $\alpha_M\beta 2$ (CD11b/CD18) is stored in cytoplasmic granules. This allows rapid up-regulation of integrin on the surface by granule exocytosis after stimulation (19). Myo1f-deficient neutrophils exhibited hyperinduction of cell-surface $\beta 2$ integrin upon stimulation with integrin ligands (ICAM-1 and fibronectin) (Fig. 3A), although total cell levels of $\beta 2$ integrin expression were comparable in wild-type and Myo1f-deficient cells (fig. S3). In

addition, this up-regulation was specific for proteins in granules, because no difference was observed in the surface expression of the neutrophil marker Gr-1, which is not known to associate with neutrophil granules (fig. S4). The release of lactoferrin, a marker for the specific granules in which a large portion of integrin $\alpha_M\beta 2$ is stored (19), is also significantly augmented in Myo1f-deficient cells upon stimulation with ICAM-1 and fibronectin (Fig. 3B). Thus, in the absence of Myo1f, increased granule exocytosis induced by integrin ligands leads to augmented $\beta 2$ integrin on the cell surface, making neutrophils more adherent.

To examine the migratory properties of neutrophils, *N*-formyl-Met-Leu-Phe (*f*MLP)-gradient chemotaxis was measured by time-lapse microscopy. When observed on polylysine-

coated glass, migration rates and efficiencies of wild-type and Myo1f-deficient neutrophils were similar (Fig. 3, C and E; fig. S5; and movies S1 and S2), in contrast to *Dictyostelium* myosin I mutants, which displayed low migration efficiency because of frequent turning (20). However, the migration rate of Myo1f-deficient neutrophils was severely impaired on fibronectin (Fig. 3D), with most neutrophils remaining attached on fibronectin (Fig. 3F and movies S3 and S4). These results suggest that, although the machinery for migration is intact in the absence of Myo1f, the increased integrin level on the surface makes these neutrophils more adherent and less motile (21).

To further explore the molecular basis of augmented granule exocytosis in Myo1f-deficient cells, we examined the intracellular location of Myo1f. Myo1f co-localizes with cortical actin filaments at the rim of the cells (Fig. 4A), and there is little co-localization with lactoferrin, which is a marker for neutrophil granule (fig. S6A). The low levels of diffuse staining in the cytoplasm are probably nonspecific, because this phenomenon is also observed on the KO neutrophils. Class I myosins in *Dictyostelium* and in yeast interact with the actin remodeling complex. Quantification of F-actin showed that there was a small but significant reduction in the amount of polymerized actin of resting neutrophils in the absence of Myo1f, whereas chemotaxis-related (*f*MLP-induced) actin polymerization was not affected (Fig. 4B), suggesting differential regulation of these actin structures (22). Cortical actin filaments near the plasma membrane, which constitute most of the F-actin in resting cells, can work as a barrier to granule secretion (23). Thus, it is possible that Myo1f indirectly inhibits granule exocytosis by modulating cortical actin. It is also possible that Myo1f exerts a direct opposing force by associating with granules. If so, this process would presumably occur as granules move into the cortex before exocytosis, because there was little co-localization of Myo1f with cytoplasmic granules even in cells that were stimulated for 7 min (fig. S6B). However, the cortical "rim" staining of Myo1f in activated cells is somewhat discontinuous and more diffuse, suggesting that there is some redistribution of Myo1f upon stimulation (fig. S6B).

Neutrophils play a crucial role in the early phase of protection against infection by *L. monocytogenes* (24). To test the effect of the phenotype described above in vivo during infection, wild-type and Myo1f-KO mice were challenged with *Listeria*. On day 2 after infection, Myo1f-KO mice contained 35 times more colony-forming units (CFUs) of *Listeria* than did wild-type littermate controls (Fig. 4C). In contrast to the well-formed microabscesses in wide-type mice (25) (Fig. 4D), poorly formed microabscesses in KO mice exposed large areas of infected hepatocytes (pale pink areas in Fig.

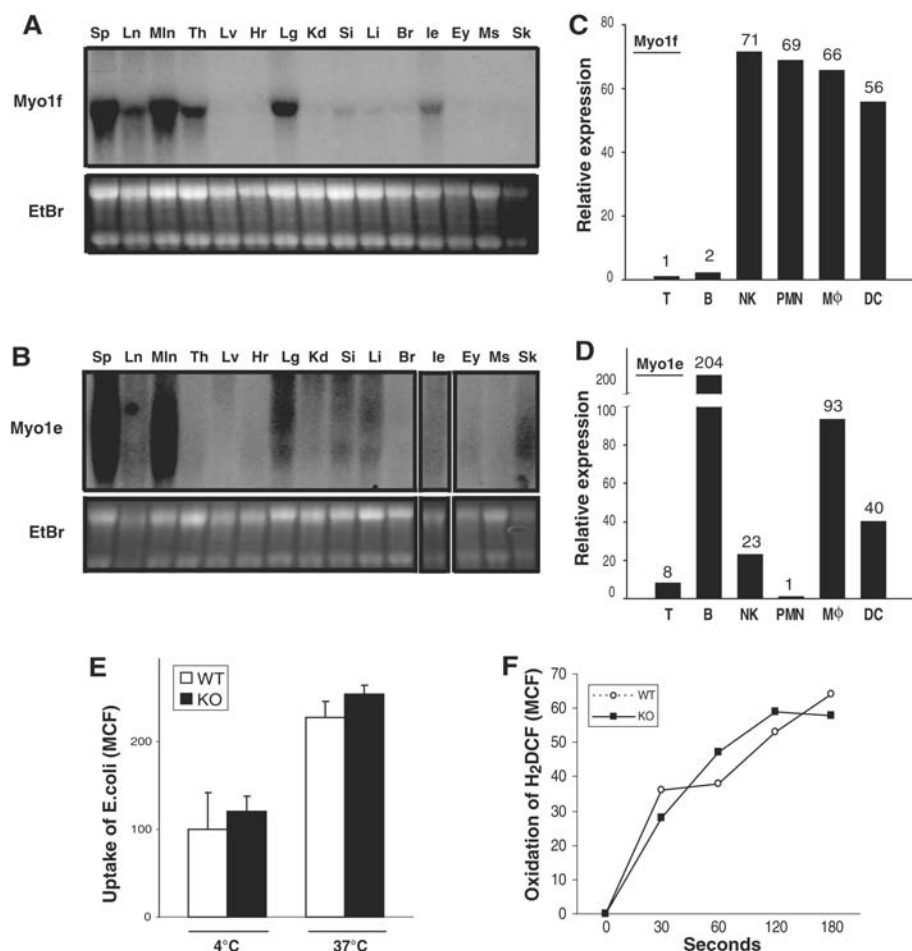


Fig. 1. Myo1f is expressed predominantly and differentially in the immune system. (A and B) mRNA levels of Myo1f (A) and Myo1e (B). EtBr, ethidium bromide. Sp, spleen; Ln, lymph node; Mln, mesenteric lymph node; Th, thymus; Lv, liver; Hr, heart; Lg, lung; Kd, kidney; Si, small intestine; Li, large intestine; Br, brain; Ie, inner ear; Ey, eye; Ms, muscle; Sk, skin. Relative mRNA levels of Myo1f (C) and Myo1e (D) in different cell types of the immune system determined by real-time reverse transcription polymerase chain reaction. T, T cells; B, B cells; NK, NK cells; PMN, neutrophils; MΦ, macrophages; DC, dendritic cells. Relative expression levels are displayed as a number on top of each bar. (E) IgG-mediated phagocytosis. Neutrophils were incubated with IgG-opsonized, fluorescein isothiocyanate (FITC)-labeled *Escherichia coli* at 37°C. Control neutrophils were incubated at 4°C. MCF, mean channel fluorescence; WT, wild type. Error bars represent SD of the mean. (F) The production of reactive oxygen species.

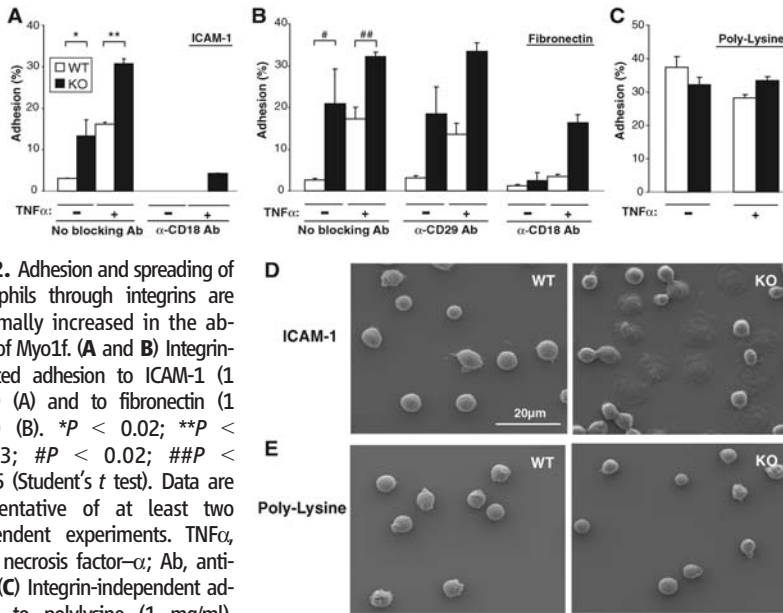
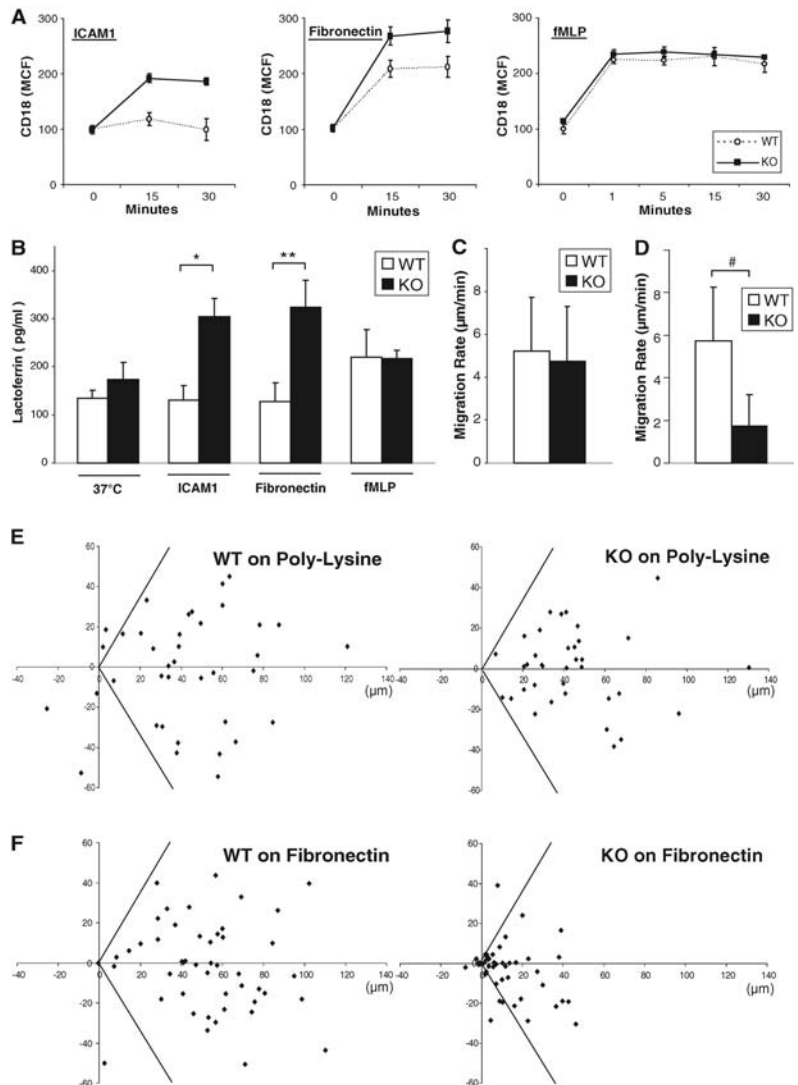


Fig. 2. Adhesion and spreading of neutrophils through integrins are abnormally increased in the absence of Myo1f. (A and B) Integrin-mediated adhesion to ICAM-1 (1 μ g/ml) (A) and to fibronectin (1 μ g/ml) (B). * $P < 0.02$; ** $P < 0.0003$; # $P < 0.02$; ## $P < 0.0005$ (Student's t test). Data are representative of at least two independent experiments. TNF α , tumor necrosis factor- α ; Ab, antibody. (C) Integrin-independent adhesion to polylysine (1 mg/ml). Error bars in (A) to (C) represent SD of the mean. (D) Spreading of neutrophils to ICAM-1 (1 μ g/ml), observed by SEM. (E) Surface morphology of neutrophils attached to polylysine (1 mg/ml), determined by SEM.

Fig. 3. In the absence of Myo1f, granule exocytosis is augmented, resulting in more $\beta 2$ integrin on the surface and impaired migration on the extracellular matrix. (A) Neutrophils were stimulated with plate-bound ICAM-1 (1 μ g/ml) or plate-bound fibronectin (1 μ g/ml) or fMLP (10 μ M) for the indicated times. Surface levels of $\beta 2$ integrin (CD18) were represented by MCF, with fluorescence of WT neutrophils at 0 min given a value of 100 units. Data are representative of three independent experiments. (B) Secreted lactoferrin was measured in the supernatant at 30 min after stimulation. * $P < 5 \times 10^{-6}$; ** $P < 5 \times 10^{-5}$ (Student's t test). Data are representative of two independent experiments. (C to F) Time-lapse video microscopy was used to examine neutrophil migration (movies S1 to S4) on polylysine (1 mg/ml) [(C) and (E)] or fibronectin (1 μ g/ml) [(D) and (F)]. The relative position of each cell is shown as a diamond in the graphs [(E) and (F)] after 10 min of migration under a 10 μ M fMLP gradient, assuming that the initial position of the cells was at (0, 0) in an xy plane. Lines with 120 $^\circ$ of arc show the area facing the source of fMLP. Data are combined from six independent experiments. (C) and (D) Average migration rate of neutrophil on polylysine (C) and fibronectin (D). # $P < 3 \times 10^{-14}$ (Student's t test). Error bars in (A) to (D) represent SD of the mean.



4E), indicating that the decreased ability to control *Listeria* is due to a defect in neutrophil mobilization. To further confirm that this in vivo defect is neutrophil-autonomous, we adoptively transferred wild-type and Myo1f-KO neutrophils into normal mice infected with *Listeria*. Myo1f-KO neutrophils were found in lower numbers in the recipient livers as compared to the observations in recipients of wild-type neutrophils (Fig. 4F), suggesting that the motility of neutrophils in vivo is compromised in the absence of Myo1f.

In accordance with the reported similarity between *Dictyostelium* and mammalian neutrophils (26), we observed that long-tailed class I myosin is conserved in cells from two different genera and supports cell motility. However, our results indicate that the ways in which myosin contributes to cell migration in the two models are quite different. Although long-tailed class I myosin in *Dictyostelium* prevents lateral pseudopod formation during migration (20), Myo1f in neutrophils inhibits exocytosis of integrin-containing granules, thereby preventing excess

adhesion. Unlike protozoan cells, metazoan cells use integrins to interact with other cells and with the environment (27). Thus, our results suggest that, in higher organisms, long-tailed myosins

have evolved to accommodate and make the best use of integrins to support cell motility. Our work also demonstrates that seemingly closely related myosin motors have different functions.

Whereas short-tailed class I myosins facilitate vesicular transport (8, 9), the long-tailed form Myo1f negatively regulates granule exocytosis in neutrophils. This work should lead to a better understanding of human immune defects that are currently of unknown origin and may provide an additional class of therapeutic targets for treating acute inflammation.

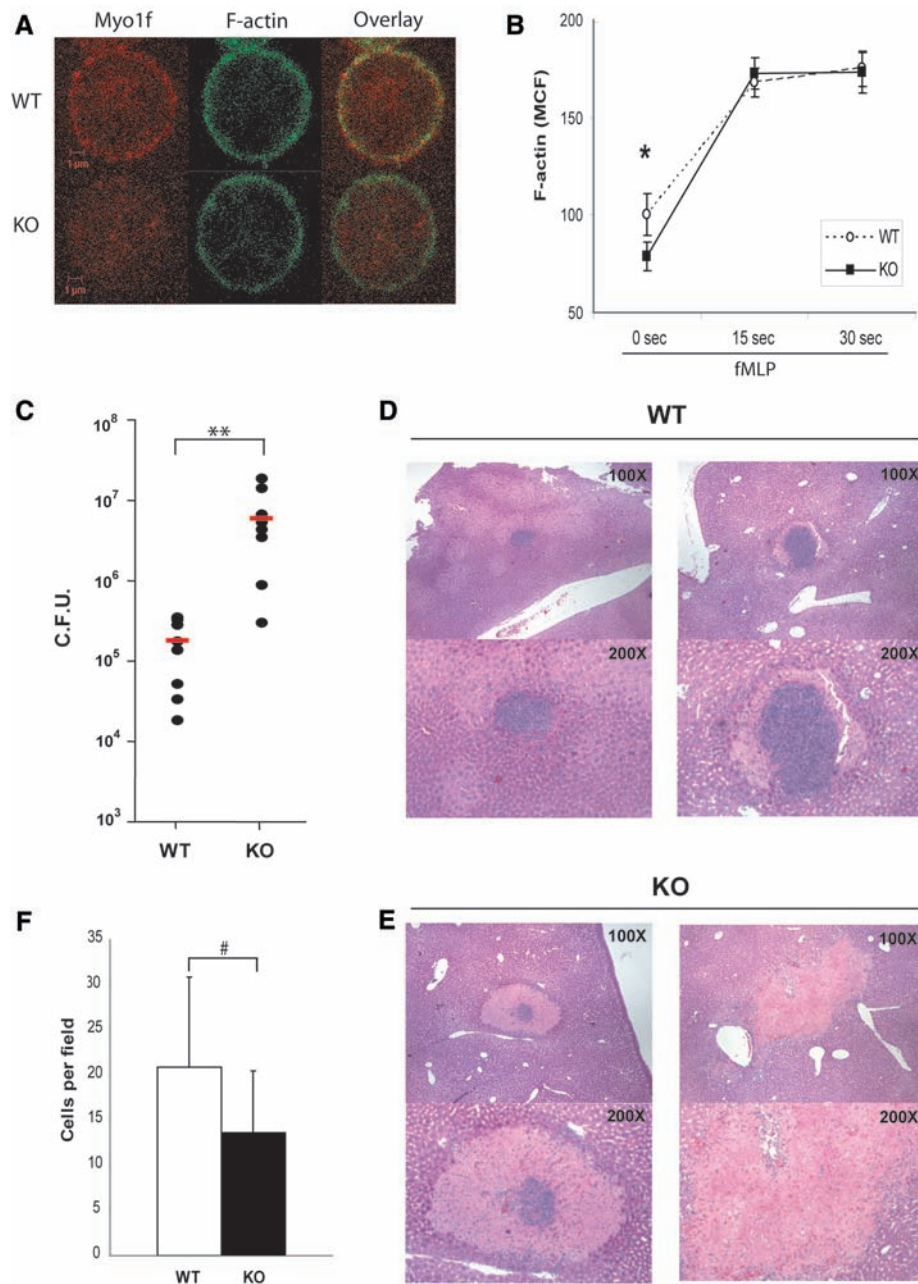


Fig. 4. Myo1f co-localizes with the cortical actin network, and neutrophil-dependent restriction of *L. monocytogenes* infection in vivo is impaired in the absence of Myo1f. (A) Confocal microscopy of neutrophils stained with antibody to Myo1f (red) and phalloidin for F-actin (green). (B) Quantification of F-actin in neutrophils after stimulation with 10 μ M fMLP. MCF was used to quantify F-actin in neutrophils after staining with FITC-phalloidin, with fluorescence of WT neutrophils at 0 min given a value of 100 units. * $P < 6 \times 10^{-5}$ (Student's *t* test). (C) The number of *L. monocytogenes* in the spleen of WT ($n = 8$) and Myo1f KO ($n = 9$) mice observed 2 days after infection. ** $P < 0.012$ (Student's *t* test). Red bars indicate mean values. (D and E) Microabscess formation in the liver of WT (D) and Myo1f KO (E) mice at 24 hours after infection. Cells with the strong blue color are neutrophils, and pale pink cells are infected hepatocytes undergoing apoptosis (25). (F) Adoptive transfer of neutrophils into mice infected with *Listeria*. The number of neutrophils localized in the liver was counted. # $P < 5 \times 10^{-9}$ (Student's *t* test). Error bars in (B) and (F) represent SD of the mean.

References and Notes

1. J. S. Berg, B. C. Powell, R. E. Cheney, *Mol. Biol. Cell* **12**, 780 (2001).
2. M. Krendel, M. S. Mooseker, *Physiology* **20**, 239 (2005).
3. M. J. Redowicz, *Acta Biochim. Pol.* **49**, 789 (2002).
4. T. A. Richards, T. Cavalier-Smith, *Nature* **436**, 1113 (2005).
5. M. A. Titus, *J. Eukaryot. Microbiol.* **47**, 191 (2000).
6. A. E. Y. Engqvist-Goldstein, D. G. Drubin, *Annu. Rev. Cell Dev. Biol.* **19**, 287 (2003).
7. J. R. Holt et al., *Cell* **108**, 371 (2002).
8. M.-N. Cordonnier, D. Dauzonne, D. Louvard, E. Coudrier, *Mol. Biol. Cell* **12**, 4013 (2001).
9. A. Bose et al., *Nature* **420**, 821 (2002).
10. M. J. Tyska et al., *Mol. Biol. Cell* **16**, 2443 (2005).
11. H. E. Stoffler, C. Ruppert, J. Reinhard, M. Bahler, *J. Cell Biol.* **129**, 819 (1995).
12. J. A. Swanson et al., *J. Cell Sci.* **112**, 307 (1999).
13. A. H. Chen et al., *Arch. Otolaryngol. Head Neck Surg.* **127**, 921 (2001).
14. T. Taki et al., *Oncogene* **24**, 5191 (2005).
15. F. Crozet et al., *Genomics* **40**, 332 (1997).
16. C. Wayne Smith, in *Clinical Immunology Principles and Practice*, R. R. Rich, T. T. Fleisher, W. T. Shearer, B. L. Kotzin, H. W. Schroeder, Eds. (Mosby, St. Louis, MO, 2001), pp. 2.22.21–15.
17. V. J. Thannickal et al., *J. Biol. Chem.* **278**, 12384 (2003).
18. K. D. Novak, M. D. Peterson, M. C. Reedy, M. A. Titus, *J. Cell Biol.* **131**, 1205 (1995).
19. M. Faurschou, N. Borregaard, *Microbes Infect.* **5**, 1317 (2003).
20. D. Wessels, J. Murray, G. Jung, J. A. Hammer III, D. R. Soll, *Cell Motil. Cytoskeleton* **20**, 301 (1991).
21. S. P. Palecek, J. C. Loftus, M. H. Ginsberg, D. A. Lauffenburger, A. F. Horwitz, *Nature* **385**, 537 (1997).
22. S. L. Gupton et al., *J. Cell Biol.* **168**, 619 (2005).
23. R. D. Burgoyne, A. Morgan, *Physiol. Rev.* **83**, 581 (2003).
24. J. W. Conlan, R. J. North, *J. Exp. Med.* **174**, 741 (1991).
25. H. W. Rogers, M. P. Callery, B. Deck, E. R. Unanue, *J. Immunol.* **156**, 679 (1996).
26. P. J. Van Haastert, P. N. Devreotes, *Nat. Rev. Mol. Cell Biol.* **5**, 626 (2004).
27. K. H. Martin, J. K. Slack, S. A. Boerner, C. C. Martin, J. T. Parsons, *Science* **296**, 1652 (2002).
28. The authors thank C. Marks in the Center for Cellular and Molecular Imaging at Yale University for help with scanning electron microscopy (SEM), L. Evangelisti and C. Hughes for technical assistance, L. Alexopoulou for technical advice, E. E. Eynon for a critical review of the manuscript, and F. Manzo for assistance with manuscript preparation. S.V.K. is a recipient of the Richard K. Gershon pre/postdoctoral fellowship. W.Z.M. and M.D. are recipients of grants from NIH (K08 DK02965 and R01 GM72002, respectively). M.S.M. is supported by grants from NIH (R01 DK25387 and R01 GM073823). R.A.F. is an Investigator of the Howard Hughes Medical Institute.

Supporting Online Material

www.sciencemag.org/cgi/content/full/314/5796/136/DC1
 Materials and Methods
 Figs. S1 to S6
 References
 Movies S1 to S4

29 June 2006; accepted 25 August 2006
 10.1126/science.1131920